

Prospects for the ultimate energy density of oxide-based capacitor anodes

Joachim Hossick-Schott
Medtronic Energy and Components Center
Medtronic Energy and Components Center, 6800 Shingle Creek Parkway, Brooklyn Center,
MN 55430
T: (001)(763) 514 0926; F: (001)(763) 514 0899; e-mail: joachim.hossick-schott@medtronic.com

Abstract

The relation between dielectric breakdown and active energy density in oxide-based capacitor systems is discussed. Of central importance for the discussion is a recently published thermochemical model predicting that the breakdown field in dry, furnace grown metal-oxide systems decreases with increasing dielectric constant. The prediction of this model is compared with experimental data collected for wet, electrolytic dielectric systems. The comparison strongly suggests that the breakdown field in dry, furnace-grown systems is equivalent to the anodization field in wet electrolytic systems. Both breakdown in furnace-grown dielectrics and oxide-growth in wet dielectric systems are likely driven by the local Lorentz-field causing molecular distortion, weakening and ultimately breakage of the chemical bonds. This local electric field is higher than the nominally applied electric field and it rises together with the increasing dielectric constant. A direct consequence of the relationship between breakdown field and dielectric constant is that the active energy density of oxide-based capacitor dielectrics is fundamentally limited. Neglecting packaging concerns, the ultimate active energy densities are predicted for intrinsic oxides with a lower dielectric constant such as silica.

Introduction

Implantable cardioverter-defibrillators are designed to restore a normal heart rhythm by providing life-saving electrical pulse therapies. A strong pulse carrying about 10 – 40 J of energy at potential differences of 600 to 800 V is transmitted directly into the heart tissue upon detection of severe arrhythmia. High-voltage capacitor technology is of paramount importance for enabling this life-preserving therapy. Two liquid electrolyte technologies, one based upon etched and stacked Al plates (1, 2), the other on pressed and sintered Ta powder (3, 4) as anode materials, are currently in use in the defibrillator industry. Ceramic capacitors have been considered for use in implantable defibrillators (5).

Patient comfort and ease-of-implant benefit from a small overall device volume. The therapy-delivering energy storage capacitor is one of the larger components inside the device as it occupies about 30 % of the implanted device volume. Hence, minimizing the volume and thereby increasing the stored energy density of this capacitor is of critical importance. Therefore, the primary intent of this contribution is to understand how much energy can be stored in a standard volume of a given material system. Packaging concerns are not addressed, only the energy stored in the dielectric, i.e., the active energy density, is of

interest. The nature of the processes that limit energy storage is also addressed. The discussion will be restricted to metal-oxide-type dielectric layers. First, a brief overview on the subject of energy storage in capacitors will be given. This will be followed by a brief characterization of the relevant dielectric material systems.

Energy storage in capacitors

$$U_{\text{stored}} = \frac{1}{2} C \cdot V^2 \quad [1]$$

Where:

U_{stored} is the stored energy (J)
 V is the applied potential difference (V)
 C is the capacitance

$$C = \epsilon_0 \cdot \epsilon_r \cdot A / d \quad [2]$$

Where:

C is the capacitance (F)
 ϵ_0 is the permittivity of vacuum ($8.8542 \cdot 10^{-12}$ F/m)
 ϵ_r is the relative dielectric constant
 A is the accessible surface area (m^2)
 d is the thickness of the dielectric (m)

$$U_{\text{stored/vol}} = \frac{1}{2} \epsilon_0 \cdot \epsilon_r \cdot E_{\text{bd}}^2 \quad [3]$$

Where:

$U_{\text{stored/vol}}$ is the stored energy per unit volume (J/m^3)
 E_{bd} is the breakdown field (V/m)

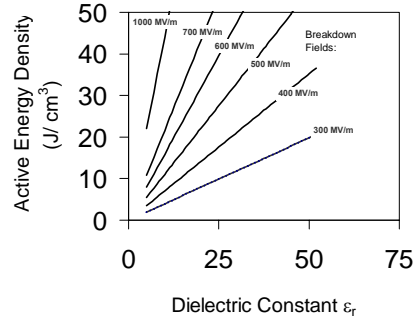


Figure 1. Active energy density as a function of the dielectric constant for various breakdown fields E_{bd} .

The energy that can be stored in an electrolytic capacitor depends upon the capacitance C and the square of the potential difference applied across the dielectric layer coating the anode. It is given in equation [1]. The capacitance C in this equation is proportional to the relative dielectric constant, the accessible surface area and the inverse of the dielectric thickness. It is given by equation [2]. Inserting [2] into [1] and normalizing the result by a standard volume yields equation [3] for the stored energy per unit volume, $U_{\text{stored/vol}}$. This entity is also known as the active energy density. This equation teaches that the active energy density depends only upon the relative dielectric constant and the square of the maximum sustainable electrical field in the dielectric material. This field is known as the breakdown field. It may be defined as the field in which the dielectric material loses its electronically insulating properties. As ionic motion is involved, the dielectric material is rendered irreversibly modified upon exposure to the breakdown field. Strategies towards increasing

the active energy density should simply consist of maximizing the breakdown field strength and dielectric constant of the material. If it were possible to increase the dielectric constant of a given material without affecting its breakdown field appreciably, very high active energy densities of $50 \text{ J} / \text{cm}^3$ or more would be achievable. This is shown in Figure 1, which is a graphic representation of equation [3].

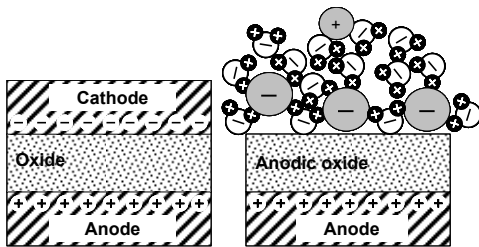


Figure 2. Dry and wet dielectric systems. a.) dry system. b.) wet system with aqueous electrolyte adjacent to the dielectric oxide layer.

III. Wet and dry dielectric systems

Generally, dielectric systems are classifiable into dry and wet materials systems. Pioneering work on anodic oxide growth and breakdown in wet, aqueous metal-oxide-electrolyte systems was performed by Güntherschulze and Betz (6) and Young (7). Recent advances in this area were reviewed by Parkhutik et al. (8), Simkins et al. (9) and Schultze and Lohrengel

(10). A comprehensive discussion of dry systems was given by Klein (11). Sketches of dry and wet systems are presented in Figure 2: In dry systems, the dielectric is sandwiched between two electronically conductive layers serving as anode and cathode. In wet systems, the dielectric interfaces with an anodically polarized electronic conductor on one side. On the other side, the cathode is constituted by an anion-rich phase in the electrochemical double layer. Wet systems may be further classified into systems with and without a pre-existing anodic oxide layer (9). An electric field may be established in all of these systems under either galvanostatic or potentiostatic conditions. Evidently, potentiostatic conditions require an existing insulating oxide. Breakdown under potentiostatic conditions may occur upon prolonged exposure of the oxide to electric fields equal to or lower than the nominal breakdown field. In wet electrolytic systems it may be induced, for example, by oxide crystallization phenomena (12, 13). In contrast, under galvanostatic conditions, breakdown occurs always at the breakdown field, in any given dry or wet system. This is sketched in

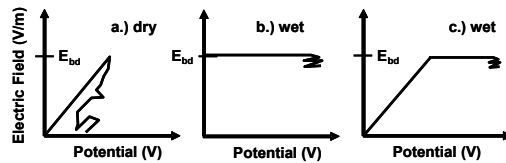


Figure 3. The electric field in the dielectric as a function of the potential difference across the dielectric layer under galvanostatic conditions. E_{bd} denotes the breakdown field. a.) Dry system. The field rises until the breakdown field is reached. b.) Wet system without a pre-existing anodic oxide layer. The field remains constant at breakdown strength until the oxide-electrolyte system breaks down. c.) Wet system with a pre-existing oxide layer. Initially, the field rises as in dry systems until the breakdown field is reached. At this constant field strength, more oxide may grow until finally the oxide-electrolyte system breaks down as under b.

Figure 3. Parasitic effects such as oxide dissolution in aggressive electrolytes and oxide contamination are not accounted for in Figure 3. For a detailed discussion of these effects, the reader is referred to the review by Parkhutik et al (8).

III a. Breakdown in dry systems

In dry systems (Figure 3a), the electric field increases until dielectric breakdown occurs. It is generally assumed that Fowler-Nordheim tunneling promotes initial

electrons into the conduction band of the dielectric; in very thin dielectrics and at higher temperatures, direct tunneling and thermal electron injection, respectively, may also contribute significantly to electron injection into the conduction band (11). The solid state cathode is the source of the electrons. Once in the conduction band, these electrons may be accelerated and generate secondary electrons and holes via impact ionization processes. A conductive percolation path may be established and physical damage may be incurred in the oxide layer at or near the anode-oxide interface (14).

III b. Breakdown in wet systems

In wet systems without a pre-existing oxide layer (Figure 3b), anodic oxide is produced upon applying a constant current. The electric field remains constant at anodization field strength until the oxide-electrolyte system reaches a certain thickness at which the oxide-electrolyte finally breaks down. Hence, the anodization field strength is identical to that of the breakdown field. Upon charging a wet system with a pre-existing anodic oxide layer (Figure 3c) the electric field rises initially, as it does in dry systems. Oxide growth under constant field conditions system will commence upon reaching anodization field strength. Eventually, breakdown occurs. It is interesting to note that the oxide-electrolyte system does break down after supporting oxide growth at breakdown field strength. In classic, so-called valve-metal systems like Ta/Ta₂O₅ or Al/Al₂O₃, anodic oxide growth is observed for considerable amounts of time (6). The resulting oxide thicknesses are often on the order of several

$$E_{loc} = [(2+\epsilon_r)/3] \cdot E \quad [4]$$

Where:

E_{loc} is the local electric field (V/m)
 ϵ_r is the relative dielectric constant
 E is the externally applied electric field (V/m)
and $E = U / d$
 U is the applied potential difference (V)
 d is the dielectric thickness (m)

hundred nanometers. The final breakdown of oxide-electrolyte systems is commonly ascribed to an electronic avalanche effect adapted from the breakdown mechanisms in dry systems (11, 14). According to Albella et al. (15), electrons may be injected into the oxide conduction band via Fowler-Nordheim tunneling from electrolyte-supplied anions. The latter are likely specifically adsorbed at the oxide electrolyte interface (16-21). Amplified by impact ionization, the propagating electron avalanche induces localized Joule-heating and damage, specifically at the metal-oxide interface. Eventually, a conductive path through the oxide is generated. The avalanche-mechanism explains nicely the observation that oxide-electrolyte breakdown is more likely in thicker oxides, simply because the electron avalanche is amplified by impact ionization and can gain more strength in thicker oxides.

The electric field and its relation to breakdown, oxide growth and energy storage

The electric field is the key for initiating and amplifying the electronic current, which is thought to ultimately cause breakdown in dry and wet oxide-electrolyte systems. Perhaps more importantly, the electric field is also the main driving force for directly distorting and breaking the chemical bonds in the oxide layer, without the aid of electronic current-induced impact ionization effects. This was pointed out in a recent thermochemical description of dielectric breakdown in dry, furnace grown oxide systems by McPherson et al. (21, 22, 23). In highly ordered dielectric systems, the electric field E_{loc} experienced locally by the charged electronic and ionic entities is a superposition of the externally applied electric field and the dipolar field establishing itself in the molecular environment. In the amorphous systems relevant for this discussion, local fields are present, because symmetry in the metal-oxide bonds is locally preserved (16, 22). This field, also known as the local Lorentz field, is given in equation [4]. The Lorentz field increases with the dielectric constant and reduces the activation energy necessary for bond breakage. In an increasing local field, the probability for bond breakage follows Boltzmann statistics: the stronger the local field becomes, the more the chemical bonds in the dielectric are weakened, distorted and rendered prone to breakage. In turn, bond breakage results in two singly charged, unpaired metal-oxygen bonds. One of the two misses an oxygen atom and is hereafter labeled (MO+), the other misses a metal atom and is labeled (MO-). If enough bonds are broken, a conductive path is established and dielectric breakdown occurs. The thermochemical model by McPherson et al. predicts that the breakdown field becomes a function of the dielectric constant (approximation [5]):

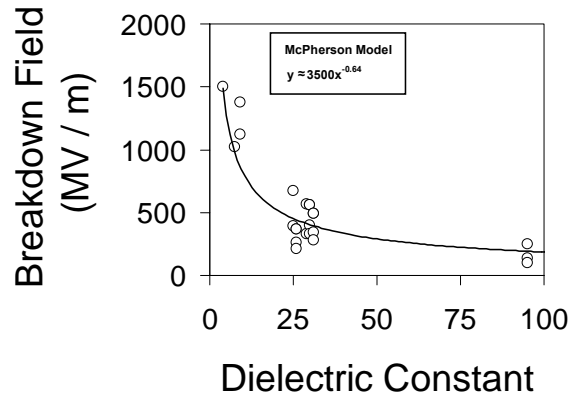


Figure 4. The relation between breakdown strength and dielectric constant as predicted by the thermochemical model by McPherson et al. (21, 22, 23). The individual data points are the result of calculations using the thermochemical model. The continuous line is a power-law fit through the data points. Multiple breakdown fields for a given dielectric constant originate from different local symmetries of the corresponding metal-oxide material.

$$E_{bd} \approx 3500 \cdot \epsilon^{-0.64} \quad [5]$$

The prediction is shown in Figure 4. It was demonstrated to correlate well with experimental data obtained on furnace grown, dry oxide systems (23). The data points in Figure 4 correspond to breakdown fields calculated with the thermochemical model for a given dielectric constant and for a given local symmetry of the oxide. Multiple points occur for a given dielectric constant or, in other words, for a given material because many oxides are known to express in different symmetries. With respect to the vector of the local electric

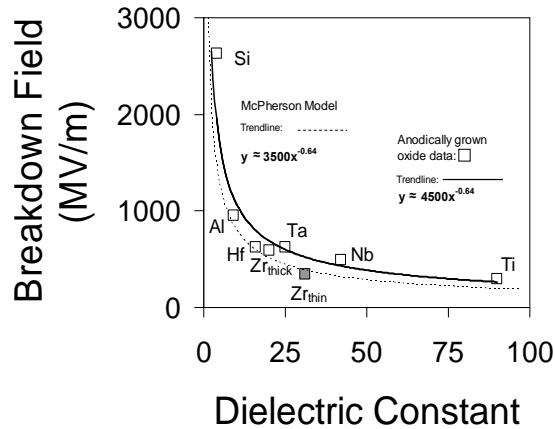


Figure 5. The breakdown strength as a function of the dielectric constant as deduced from experimental data. The solid line represents a trendline fitted to experimental data obtained from the literature. Materials and references: Si (30); Al (25); Hf (27); Zr_{thick} (28); Zr_{thin} (29); Ta (26); Nb (31); Ti (32). The data point for thin zirconium oxide (~ 10 nm) is not included in the trend line calculation. The dotted line is the prediction of the thermochemical model by McPherson et al. (21,22, 23).

field, the local symmetry decisively determines if the bond is going to be stretched – and rendered prone to breakage – or compressed by the local field. Thus, the thermochemical model explains breakdown without invoking electronic current- and impact ionization effects. However, McPherson et al. did show that the field-induced bond distortions may be combined with electronic current effects such as hole-capture resulting from impact ionization (24). Hole-capture serves to catalyze the thermochemical bond-breakage process and renders chemical bonds, in the vicinity of the oxide-anode interface, more prone to breakage. But even without invoking electron-current-related effects, the model appears to work very well in dry systems. But - what about wet systems? Oxide-electrolyte systems support oxide growth at breakdown field strength for prolonged amounts of time until they finally break down. The oxide growth process is often characterized by the thickness increase per Volt of applied potential difference (7). This quantity is known as the oxide growth rate and is typically quoted in nm per V (nm/V). For example, Al_2O_3 grows about 1.1 nm per Volt (25), Ta_2O_5 with 1.6 nm per Volt (26). This growth rate does vary somewhat as the oxide thickness increases, but these variations typically appear together with variations in the dielectric constant (see, e.g., the data for the oxide of Zr in Figure 5). The growth rate and the dielectric constant may also change somewhat with the pH, the current density and the anion species in the electrolyte (see, e.g., reference (27)). Overall, however, these variations may be considered small, specifically if chemical effects such as oxide dissolution in particular electrolyte chemistries are neglected. The inverse of the oxide growth rate has the dimension of an electric field and is called the anodization field of a given oxide species. Based on the discussion in chapter III b, one may speculate if the thermochemical model of McPherson et al. predicts the anodization field strength in wet systems. Indeed, Vijn (33) similarly proposed that the anodization field increases with increasing metal-oxide bond strengths. Figure 5 represents a test of this speculation: It shows the anodization fields of several oxide-electrolyte systems as a function of their dielectric constants. The data are collected from the literature, as indicated in the caption of Figure 5. Evidently, the trend predicted by the thermochemical model for furnace-grown oxides is valid also for anodically grown oxides. The exponent in the power laws stated in the inserts of Figure 5 for anodic oxides and furnace-grown oxides is identical; the pre-exponential factor is somewhat different. This difference may be related to the fact that different local symmetries may occur in anodic and furnace-grown oxides. It may also simply be due to uncertainties in the thickness-measurement of the anodic oxides. The fact that anodic oxide growth and breakdown of dry oxide systems appear to be related may be surprising at first glance. Not so upon further examination (see Figures 6 and 7). The model of McPherson et al. proposed bond breakage in (dry) oxide systems exposed to the breakdown strength of the electric field. For anodic oxide growth, Odynets (16) proposed a mechanism that essentially also invokes broken bonds. Odynets labeled them “vacancy” bonds. He did so in account of the fact that classic, ionic point defects are unlikely to occur in metal-oxide bonds with a high degree of covalence. According to Odynets (16), the probability for the creation of “vacancy” bonds would be highest at the metal-oxide and the oxide-electrolyte interfaces. Likewise with the thermochemical model: the probability for bond-breakage at a given electric field strength would likely be highest in the interfacial areas since the metal-oxide bonds there are likely the weakest. A vacancy bond owned by an oxygen atom with a metal atom missing would be negatively charged (labeled MO^-) and a vacancy bond owned by a metal atom with an oxygen atom missing would be positively charged (labeled MO^+). Following Odynets further, bond migration via bond switching is possible in the electric field. (MO^+) bonds would then migrate from the metal-oxide interface to the oxide-electrolyte interface. (MO^-) bonds would go in the opposite direction. Odynets argued that upon arrival of a (MO^+) bond at the oxide-electrolyte interface, dissociative adsorption of a water molecule would supply

the oxygen for a new oxide molecule and / or the creation of new (MO-) bonds (see Figure 6a, left). In a subtle variation, the thermochemical model proposes instead that a metal-oxide bond at the oxide-electrolyte interface ruptures, leaving behind both (MO+) and (MO-) bonds (see Figure 7a, left). A new metal-oxygen bond is established upon dissociative adsorption of water on the metal atom of the (MO+) bond. Subsequently, the (MO-) bond may migrate to the metal-oxide interface to recombine there with a metal atom. At the metal-oxide interface, Odynets (16) proposed further that oxygen may be removed from the oxide layer via reaction with the underlying metal substrate atoms, thereby creating new oxide molecules and new (MO+) bonds (see Figure 6a, right). Again in subtle variation, the thermochemical model proposes a ruptured bond at the metal-oxide interface, leaving (MO+) and (MO-) bonds behind (see Figure 7a, right). The (MO-) bond may create new oxide by reacting with the underlying metal; the (MO+) may migrate to the oxide-electrolyte interface (see Figure 6b and 7b). Thus, both, the model of Odynets (16) and the thermochemical model do explain oxide growth occurring at the oxide interfaces. The models also explain the generation of a continuous supply of (MO-) and (MO+) bonds serving as carriers for oxygen

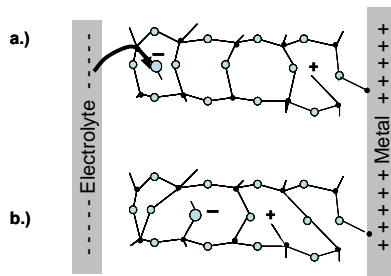


Figure 6. Bond-switching model for metal-oxides in an electric field, after Odynets (8). Larger, open circles; oxygen sites. Small, full circles; metal sites. a.) Vacancy-bonds are created at the oxide-electrolyte and the metal-oxide interfaces. On the electrolyte side, the arrow denotes oxygen supply from the electrolyte via dissociative adsorption. On the metal substrate side, the formation of a (MO+) bond is initiated by the reaction of oxygen with the metal substrate. b.) The vacancy bonds migrate under influence of the field.

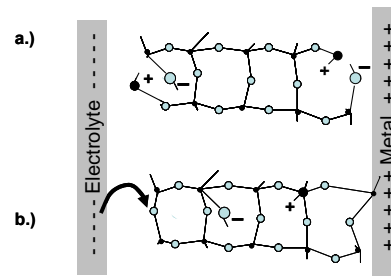


Figure 7. Bond-breaking with subsequent bond switching in an electric field, following the thermochemical model. Larger, open circles; oxygen sites. Small, full circles; metal sites. a.) Field-induced bond breakage occurs at the oxide-electrolyte and the metal-oxide interfaces. b.) As broken bonds migrate as in the Odynets model, new oxygen and metal atoms are supplied from the electrolyte and the metal substrate. Oxygen supply via dissociative adsorption is indicated by the arrow.

and metal atoms and fueling oxide growth at both interfaces. The thermochemical model may be considered a subtle variation of the model by Odynets in that (MO+) and (MO-) bonds would not occur at the oxide interfaces by way of chemical reactions. Rather, they would be generated pair-wise via bond breakage (see Fig. 7). Bond migration and the oxide creation processes at the metal-oxide and at the oxide-electrolyte interfaces would remain as envisioned by Odynets. Thus, fusing the physics-based thermochemical model by McPherson et al. with the ideas proposed by Odynets clarifies the oxide growth process. It also explains the striking similarity between the breakdown fields predicted by the thermochemical model and the anodization fields observed in various materials (Figure 5): the breakdown field of dry systems appears to be identical to the anodization field in wet systems.

Now back to equation [3] for the active energy density: Inserting the analytical relationship between the breakdown field and the dielectric constant derived from the thermochemical model (equation [5]) allows for two other important conclusions to be drawn (see Figure 8). The active energy density of electrolytic capacitors based upon metal-oxide dielectrics becomes fundamentally limited. And: The active energy density is predicted to be highest for materials with a low dielectric constant.

It should be emphasized again, that the energy density plotted in Figure 8 accounts just for the active energy in the dielectric; the volume of metal contacts needed to supply the charge for dry systems and the volume of a metal substrate and electrolyte to supply charge in wet systems - in short: any packaging volumes - are not included. Hence, Figure 8 represents the maximum active energy density theoretically possible in metal oxide capacitors. Practically achievable values will always be lower.

Importantly, McPherson et al. (21, 22, 23) discuss yet an other factor that would further

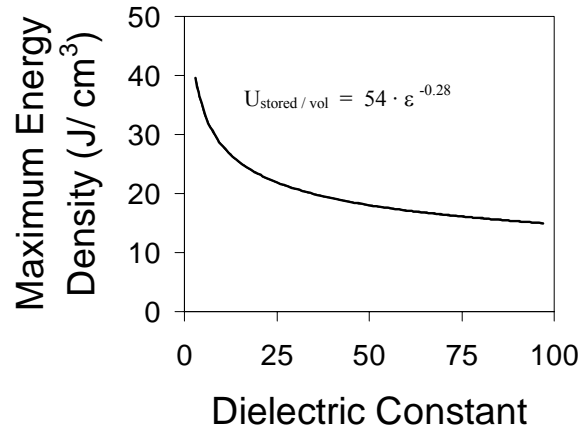


Figure 8. The maximum energy density in metal-oxide dielectric as predicted by the thermochemical model of McPherson et al. No contact or electrolyte volumes or any packaging are accounted for. The highest energy densities should be achievable with low dielectric constant materials.

diminish the theoretically achievable energy density, namely the so-called ‘time-to-failure’ observed in time-dependent breakdown experiments on dry metal-oxide systems. Following this discussion, the safe operating field for low dielectric constant materials is about 10 – 15 percent lower than the breakdown field. For high dielectric constant materials, on the other hand, the safe operating field may be a higher fraction of the breakdown field. Thus, in practice, the energy density advantage for low dielectric constant materials indicated in Figure 8 would likely not be quite as high, though it should be still noticeable. A future publication will discuss the time-to-failure aspect further.

Conclusions and Outlook

From the Figures and the discussion above, the following points appear to be the main takeaways:

- 1.) The active energy density of capacitors with metal-oxide dielectrics is fundamentally limited.
- 2.) The active energy density increases with decreasing dielectric constant.
- 3.) The breakdown field in dry dielectric systems is approximately equivalent to the anodization field in wet dielectric systems.
- 4.) The model of Odynets (16) for anodic oxide growth is validated by the thermochemical model of McPherson et al. (21, 22, 23); or, conversely speaking,

the model of Odynets validates the application of the thermochemical model in wet systems - not, however, to predict breakdown in the latter, but rather, to predict the anodization field.

- 5.) With the introduction of the thermochemical model into the models of *wet* oxide growth, it becomes possible to understand the anodic oxide growth process from a physics-based point of view. Bond-breakage by virtue of the local Lorentz-field appears to be the key driving force for anodic oxide growth.

Of course, questions immediately arise. One such question is if the thermochemical model may also be valid for non-oxide based dielectric systems. A superficial scan of available data for polymers does not yield a contradiction. Obviously, it would be of tremendous interest to generalize the thermochemical model to all possible dielectrics.

Acknowledgements

The author is indebted to Dr. Joe Mcpherson from Texas Instruments and to Dr. Paul Skarstad, retired from Medtronic, for discussing and improving the manuscript. Dr. Mark Viste and Dr. Michael Hintz, both of the Medtronic Energy and Components Center, are gratefully acknowledged for their critical comments.

References

- (1) M. Breyen, A. Rorvick, P. Skarstad, Capacitor and Resistor Technology Symposium (CARTS USA), 197, (2002)
- (2) J.L. Stevens, M.A. Moore, X. Jiang, C.R. Feger and T.F. Strange, Capacitor and Resistor Technology Symposium (CARTS USA), Proceedings, pp. 249 – 254, (2004).
- (3) D. A. Evans, US Patent #5,369,547 (1994)
- (4) A. Shah, B.C. Muffeetto, N.N. Nesselbeck, US Patent 5,894,403 (1999).
- (5) A. Rorvick, A. Crespi, J. Dougherty, E. Breval, F. Duva, 22nd Capacitor and Resistor Technology Symposium (CARTS USA), (2002).
- (6) “Elektrolyt-Kondensatoren”, A. Güntherschulze, H. Betz, M. Krayn publisher, Berlin, 1937.
- (7) “Anodic oxide films”, L. Young, Academic Press, London, New York, 1961.
- (8) V.P. Parkhutik, J.M. Albella and J. M. Martinez-Duart, Modern Aspects of Electrochemistry 23, pp. 315 – 391 (1992).
- (9) L.F. Simkins, K.B. Doyle and T.B. Tripp, 22nd Capacitor and Resistor Technology Symposium (CARTS USA), pp. 236-43 (2002).
- (10) J.W. Schultze and M.M. Lohrengel, Electrochimica Acta 45, pp. 2499 – 2513, (2000).
- (11) N. Klein, Advances in Physics, 21, pp. 605 – 645, (1972).
- (12) N.F. Jackson, J. Applied Electrochem., 3, pp 91 – 98, 1973.
- (13) L.L. Odynets, Russian Journal of Electrochemistry, 23(12), pp. 1703 – 1706 (1987).
- (14) L.C. Chen, S. Holland, C. Hu, International Reliability Physics Proceedings (IEEE), p24 (1985).
- (15) J.M. Albella, I. Montero, J.M. Martinez-Duart, Electrochimica Acta., 32(2), pp. 255 – 258 (1986).
- (16) L.L. Odynets, Materials Science Forum Vols. 185 – 188, pp. 553 – 562 (1993).

- (17) J. Hossick-Schott, M. Viste, 20th Capacitor and Resistor Technology Symposium (CARTS Europe), pp. 39-46 (2006).
- (18) C. Outhwaite, M. Molero, J. Chem. Soc., Farady Trans. 2, 85(9), pp. 1585 – 1599 (1989).
- (19) G. Horanyi, J. Colloid and Interface Science, 252, pp. 214 – 221 (2002).
- (20) G. Horanyi, G.G. Lang, J. Colloid and Interface Science, 296, pp. 1 – 8 (2006).
- (21) J. McPherson, J. Kim, A. Shanware, H. Mogul and J. Rodriguez, IEEE-IEDM Digest of Technical Papers, 633 (2002).
- (22) J. McPherson, J. Kim, A. Shanware, H. Mogul and J. Rodriguez, IEEE Transactions on electron devices, 50 (8), pp 1771 – 1778 (2003).
- (23) J. McPherson, J. Kim, A. Shanware and H. Mogul, Appl. Phys. Lett., 82(13), pp. 2121-2123 (2003).
- (24) J.W. McPherson, R.B. Khamankar, A. Shanware, J. Appl. Physics 88(9), pp. 5351 – 5359 (2000).
- (25) R.C. Furneaux, G.E. Thompson, G.C. Wood, Corros. Sci. 18 pp. 853 – 881 (1978).
- (26) J. Kleber, J. Electrochem. Soc. 132, pp. 896 - 899 (1965).
- (27) M. J. Esplandiu, E. M. Patrito, V. A. Macagno, Electrochimica Acta, 40(7), pp. 809 - 815 (1995).
- (28) Thierry Pauporte, Joergen Finne, J. Appl. Electrochemistry 36, pp. 33 - 41 (2006).
- (29) P. Meisterjahn, H.W. Hoppe, J.W. Schultze, J. Electroanal. Chem. 217, pp. 159 – 185 (1987).
- (30) P.F. Schmidt, W. Michel, J. Electrochem. Soc., 104(4), pp. 230 – 236 (1957).
- (31) L. Young, Can. J. Chemistry 38, pp. 1141 – 1147 (1960).
- (32) K.D. Allard, M. Ahrens, K.E. Heusler, Werkstoffe u. Korrosion 26(9), pp. 694 - 698 (1975).
- (33) A. K. Vijh, J. Electrochem. Soc., 116(7), pp. 972 – 975 (1969).